

Article

A Long-Term Record of Quaternary Facies Patterns and Palaeoenvironmental Trends from the Po Plain (NE Italy) as Revealed by Bio-Sedimentary Data

Veronica Rossi ^{*}, Alessandro Amorosi , Giulia Barbieri , Stefano Claudio Vaiani , Matteo Germano and Bruno Campo

Department of Biological, Geological and Environmental Sciences, University of Bologna, Via Zamboni 67, 40126 Bologna, Italy; alessandro.amorosi@unibo.it (A.A.); giulia.barbieri21@unibo.it (G.B.); stefano.vaiani@unibo.it (S.C.V.); matteo.germano5@studio.unibo.it or germat94@gmail.com (M.G.); bruno.campo@unibo.it (B.C.)

* Correspondence: veronica.rossi4@unibo.it

Abstract: Understanding Quaternary dynamics of delta-coastal plains across multiple glacial-interglacial cycles in the Milankovitch band (~100 kyrs) is crucial to achieve a robust evaluation of possible environmental response to future climate-change scenarios. In this work, we document the long-term bio-sedimentary record of core 204 S16 (~205 m long), which covers a wide portion of the post-MPR (Mid-Pleistocene Revolution) interval, taking advantage of the highly subsiding context of the SE Po Plain (NE Italy). Detailed facies characterization through an integrated sedimentological and meiofauna (benthic foraminifers and ostracods) approach allowed for the identification of a repetitive pattern of alluvial deposits alternating with four fossiliferous, paralic to shallow-marine units (Units 1–4). The transgressive surfaces identified at the base of these units mark major flooding events, forced by Holocene (Unit 4), Late Pleistocene (Unit 3) and Middle Pleistocene (Units 1, 2) interglacials. Distinct stratigraphic patterns typify the Middle Pleistocene interval, which includes coastal-marine (tidal inlet and bay) deposits. In contrast, lagoonal sediments record the maximum marine influence in the Late Pleistocene-Holocene succession. As a whole, the meiofauna tracks a regressive trend, with the deepest conditions recorded by the oldest Unit 1 (MIS 9/11 age?).

Keywords: Quaternary changes; benthic foraminifers; ostracods; Pleistocene; cyclic sedimentation; Mediterranean coastal plains



Citation: Rossi, V.; Amorosi, A.; Barbieri, G.; Vaiani, S.C.; Germano, M.; Campo, B. A Long-Term Record of Quaternary Facies Patterns and Palaeoenvironmental Trends from the Po Plain (NE Italy) as Revealed by Bio-Sedimentary Data. *Geosciences* **2021**, *11*, 401. <https://doi.org/10.3390/geosciences11100401>

Academic Editors: Emanuela Mattioli and Jesus Martinez-Frias

Received: 16 August 2021

Accepted: 17 September 2021

Published: 23 September 2021

Publisher's Note: MDPI stays neutral with regard to jurisdictional claims in published maps and institutional affiliations.



Copyright: © 2021 by the authors. Licensee MDPI, Basel, Switzerland. This article is an open access article distributed under the terms and conditions of the Creative Commons Attribution (CC BY) license (<https://creativecommons.org/licenses/by/4.0/>).

1. Introduction

Deltas and coastal plains are complex depositional systems that include a variety of mutually linked environments. These regions are sensitive to regional controls, including climate and relative sea level (RSL) conditions, but also to local factors, such as river dynamics, subsidence rates, inherited morphologies and human activities. All these processes operate over a wide range of time scales [1–5]. Under the threat of Global Change, these low-lying areas are highly exposed to severe flooding, territory loss and damage of ecosystems [6–8], making urgent a robust evaluation of the present-day state of health through monitoring techniques [9–12] and a correct quantification of the environmental-ecological quality status [13–17]. However, an improved comprehension of the depositional-environmental responses to external factors through time and space is key to produce reliable projections and conservation-restoration strategies [18]. In this scenario, only the geological perspective can furnish a long-term view on coastal and fluvial dynamics and associated forcings. Specifically, the Quaternary record represents an exceptional archive of information being only partially affected by tectonics or diagenetic processes. During the last decade, many stratigraphic-based, multiproxy studies on the Quaternary sedimentary successions of the Mediterranean plains have documented the essential role of

integrating bio-sedimentary approaches (for instance, combined malacofauna, meiofauna and palynological analysis) to track environmental changes and depositional trends. In particular, the feasibility of radiocarbon dating, and the relatively easy recovery of undisturbed, continuously cored successions allowed the detailed exploration of the Holocene record. The resulting data highlight the predominant influence of RSL rise during the Early Holocene, whereas short-term oscillations in climate, river flow regime and human impact seem to have been the main drivers of change under Mid-Late Holocene highstand conditions ([19–23] among others). Expanding the observation back to the beginning of the Late Pleistocene (ca. 130 kyrs BP), the depositional architecture preserved beneath the Mediterranean coastal plains seems to reflect the well-known 100 kyrs glacio-eustatic cyclicity (MISs 5–1). Nevertheless, river incisions driven by the last glacial RSL fall [24] can make the Pleistocene record strongly fragmented and difficult to be resolved especially under low subsidence rates and complex tectonic settings [25–29].

Despite the importance to improve our knowledge about the effects of consecutive, multiple glacial-interglacial cycles on coastal plains, scarce attention has been paid to the pre-MIS 5 deposits so far. To the best of our knowledge, facies-based stratigraphic analyses of Mediterranean successions encompassing hundreds of thousands of years are few and mostly located in the N Adriatic area–NE Italy (Po Plain and Venice Lagoon–Figure 1; [30–34]), where a relatively thick Quaternary record occurs due to favourable tectonic conditions. In particular, the southern portion of the Po coastal plain (Figure 1) represents a suitable candidate for long-term palaeoenvironmental studies, because: (i) it belongs to a rapidly subsiding basin (Po Basin: up to 2.5 mm/yr over the last 1.43 Myr; [35]), that hosts a stratigraphically expanded Quaternary succession [36,37], and (ii) a set of ~200 m long continuous cores has been recovered during the drilling campaign promoted by the Geological Survey of Regione Emilia-Romagna, contributing to the Geological Map of Italy at 1:50,000 scale (CARG Project).

This work aims to provide a bio-sedimentary record of the palaeoenvironmental dynamics affecting the SE Po Plain over a wide portion of the post-MPR (Mid-Pleistocene Revolution) interval, typified by the 100 kyrs glacio-eustatic cyclicity (last ~ 600 kyrs; [38]), through the integrated analysis of a ~205 m-thick cored succession (core 204 S16; Figure 1). Taking advantage of the high degree of preservation potential of the Po Basin, specific objectives are: (i) to furnish new insights about the evolution trends of rapidly subsiding coastal areas under the forcing of consecutive climate-RSL oscillations via facies analysis, and (ii) to reconstruct and compare long-term changes as recorded by palaeocommunities (i.e., benthic foraminifers and ostracods) along a stratigraphic profile covering hundreds of thousands of years.

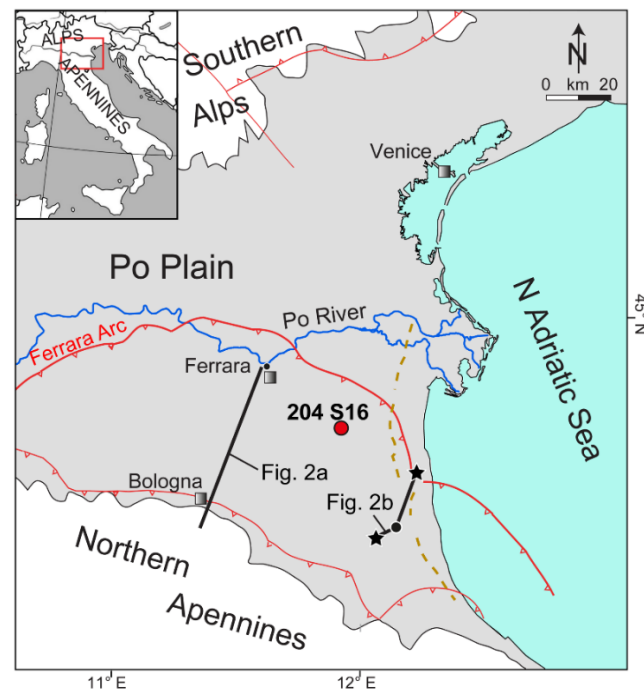


Figure 1. Location map of the studied core 204 S16 (red dot). The main Alpine and Apennine structures of the eastern sector of the Po Plain (modified from [39]) are reported along with the seismic and stratigraphic profiles showed in Figure 2a,b. Black stars indicate deep (>100 m) continuously cored boreholes cores with pollen data. The orange dotted line corresponds to the innermost outcropping beach-ridges, dated to the pre-Etruscan times (>2800 years BP) [40].

2. Study Area

2.1. Geological Context

The Po Plain is one of the most extensive (~48,000 km² wide) alluvial-coastal plains in the W Mediterranean area. It is fed by the Po River (~690 km long; [41]), which currently forms a wide multi-lobe delta system on the N Adriatic platform (Figure 1), and to a lesser extent by N Apennine rivers. The Po Plain represents the surficial expression of the peri-sutural basin (i.e., Po Basin) bounded by two mountain chains, the Southern Alps to the North and the Northern Apennines to the South (Figure 1). These orogens developed in the context of the convergence between the European and African plates since the Cretaceous [39,42]. Below the southern Po Plain, geophysical studies documented the presence of buried structures belonging to the frontal thrust system of the Northern Apennines [43]. The Ferrara arc, which affects the SE portion of the Po Plain (Figure 1), is considered to have been tectonically active since the Early Pliocene [44]. Because of its complex structural framework, vertical displacement rates strongly vary across the plain with maximum subsidence values estimated far away from the anticline culminations [45]. Bruno et al. (2020) [46] argued that buried Apennines thrust-related folds have mainly controlled the spatial distribution of subsidence rates over the last 120 kyrs in the southern Po Plain, with the secondary contribution of sediment compaction due to highly compressible depositional facies (e.g., prodelta, lagoon and swamp muds).

2.2. Stratigraphic Setting

The thickness of the Pliocene-Quaternary sedimentary infill of the Po Basin commonly ranges between few hundreds of meters in correspondence of the buried anticlines to 6–8 km in the depocenters (e.g., [43,44,47]). In the eastern part of the Po Plain, south of the Po River, seismic profiles and deep wells drilled for hydrocarbon exploration documented (Figures 1 and 2a): (i) a decreasing tectonic deformation from Pliocene to Quaternary deposits, (ii) the occurrence of six third-order depositional sequences (*sensu* [48]) bounded by regional, tectonic-driven unconformities (named A–F in Figure 2a; [49]), and (iii) an

overall regressive trend from deep-sea to continental deposits [50]. Specifically, deep-marine deposits, mainly Late Miocene–Pliocene in age (e.g., [36,50]), were replaced by coastal (Qm in Figure 2a) and continental (Qc in Figure 2a) sedimentation during the Pleistocene [49,51]. This stratigraphic architecture documents an overall tectonic control on the Po Basin infilling (e.g., [43,51]). The uppermost part of the succession (up to hundreds of meters thick), composed of Middle Pleistocene to Holocene deposits (Qc in Figure 2a) shows the cyclic alternation of alluvial and subordinate shallow-marine-paralic deposits in the distal sector of the plain [52,53]. Detailed studies on the uppermost ~100 m of the Po sedimentary succession [27] highlighted the development of two coastal wedges, forming the transgressive + highstand systems tracts (TST + HST; Figure 2b) chronologically assigned to MIS 5e (around 100–130 m below sea level-BSL) and MIS 1 (uppermost 30 m) by means of absolute ages (^{14}C , Optically Stimulated Luminescence-OSL and Electron Spin Resonance-ESR ages; [29]). Prominent Transgressive Surfaces (TSs) mark the base of these coastal bodies, separated by a tens m-thick succession of alluvial deposits corresponding to the falling-stage and lowstand systems tracts (FSST + LST; Figure 2b). Integrated pollen data from selected cores (223 S17 and 240 S13 in Figures 1 and 2b) point to a predominant glacio-eustatic control at a Milankovitch-scale (100 kyrs cyclicality). Indeed, transitional-shallow marine deposits invariably formed under interglacial conditions (i.e., high AP-Arboreal Pollen/NAP-Non Arboreal Pollen ratio), while alluvial deposits developed under glacial conditions (i.e., low AP/NAP ratio; [5,52,54]). A few studies investigated in detail the pre-MIS5e record [30,53,55], however chronologic attribution and stratigraphic correlations of these deposits remain rather uncertain across the Po Plain.

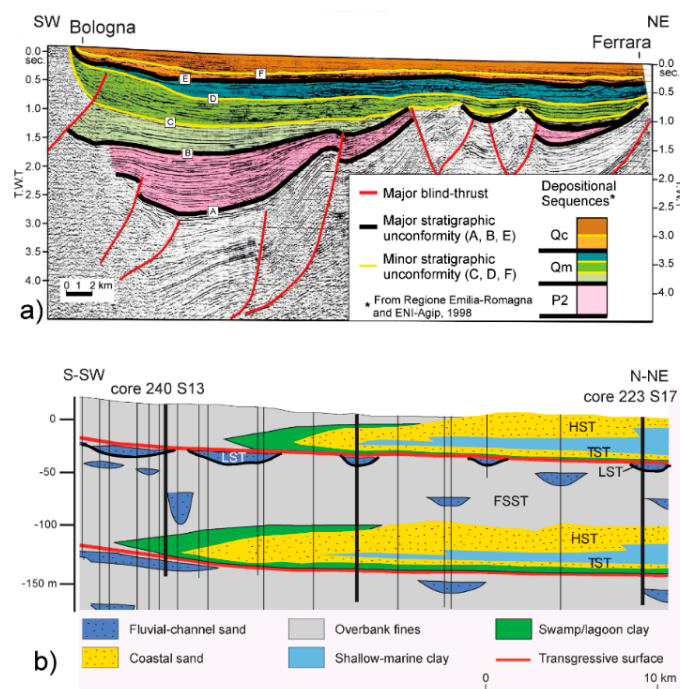


Figure 2. Stratigraphic architecture of the sedimentary infill of the Po Basin. Section traces are reported in Figure 1. (a): interpreted seismic profile showing the Pliocene (P)-Quaternary (Q) depositional sequences, related stratigraphic unconformities (A–F lines) and the major blind thrusts (red lines) as identified by [49]. T.W.T.: two-way travel time. (b): glacio-eustatic driven, cyclic sedimentation pattern of the Po coastal plain over the ~130 kyrs BP, as revealed by the facies architecture of the uppermost ~130 m (from [27]). Red lines highlight the Transgressive Surfaces (TSs) that mark the lower boundary of coastal wedges attributed to the last and present-day interglacials (MIS 1 and MIS 5e, respectively). Coastal wedges include transgressive (TST) and highstand (HST) deposits, while alluvial deposits compose the falling-stage and lowstand systems tracts (FSST + LST).

3. Materials and Methods

Integrated sedimentological and palaeobiological (benthic foraminifers and ostracods) analyses were undertaken on a long-cored succession (~205 m) recovered ~2 m below the sea level in the southern Po coastal plain (204 S16 core in Figure 1), by a continuous perforating system that guaranteed an undisturbed stratigraphy and a high recovery percentage (>95%). Core 204 S16 was drilled during the production of the Sheet 204-Portomaggiore (CARG Project; [56]). Its location, ~15 km inland the innermost outcropping beach-ridges archaeologically dated to the pre-Etruscan times (>2800 years BP from [40]; Figure 1), determined a high variability of lithofacies as interpreted by [29] for the uppermost 140 m. In this work, we additionally analysed the lower portion of the core, providing detailed bio-sedimentary data for the entire succession. The original description of core stratigraphy is available in the Emilia-Romagna Geological Survey database (Emilia-Romagna Geological, Seismic and Soil Survey, Geological cartography webgis; [57]); it includes data about sediment grain size, colour, type of contact between lithofacies and accessory elements, such as mollusc shells, peaty horizons, root traces and pedogenic features (i.e., carbonate nodules). Pocket penetrometer (PP) values are also available for the fine-grained intervals in the uppermost 100 m, furnishing information about their consistency.

Samples for micropalaeontological analyses were collected throughout the entire succession in order to characterise all the lithofacies. We mostly focused on fine-grained deposits, where the presence of other fossil remains, organic-rich layers or the stratigraphic position were suggestive of an abundant, autochthonous meiofauna. Thirty-nine samples with a weight of ~150 g were selected and treated following the standard method reported in [58] and other reference works of the study area. The procedure involved: (i) sediment oven-drying for 8 h at 60 °C; (ii) soaking in water; (iii) wet-sieving at 63 µm (240 mesh) and (iv) oven-drying again. After a preliminary screen of the obtained residue under a binocular microscope, 10 out of the 14 samples containing abundant and well-preserved meiofauna were treated with carbon tetrachloride (CCl₄) to separate foraminiferal tests through flotation and facilitate quantitative analyses. Sediment (both the floated and the heavy fractions) was dry sieved at 125 µm and divided through a microsplitter into small proportions, including at least 250 benthic foraminifers that were picked and identified; otherwise, the entire residue was analyzed. *Ammonia tepida* and *Ammonia parkinsoniana* were counted together. Benthic foraminifer counts are reported in Table S1 of the Supplementary Materials. Then, the light (floated) fraction was added to the heavy residue including grains and most of the ostracod valves, to perform a semi-quantitative observation of the ostracod fauna in relation to the abundance of benthic foraminifers and sedimentological characters of the sample (Table S2 of the Supplementary Materials). Ostracod data were expressed following three categories of relative abundance (abundant ≥ 30%, common 10–30%; scarce ≤ 10%). Identification of taxa was supported by original descriptions [59,60], as well as key works on benthic foraminifers and ostracods from modern settings [61–66] and late Quaternary coastal successions of the Mediterranean area [67–69]. The micropalaeontological samples are housed in the Department of Biological, Geological and Environmental Sciences of the University of Bologna.

In order to better highlight and compare palaeoenvironmental changes throughout the core profile, benthic foraminifers and ostracods were assigned to ecological groups, on the basis of autoecological characteristics and distribution from modern Mediterranean environments (e.g., [64,70–73] and references therein). In particular, benthic foraminiferal groups were defined mostly focusing on works of the North Adriatic area and considering environmental preferences of taxa in the microtidal Mediterranean setting. The groups are: (i) shallow marine; (ii) lagoon to shallow marine; (iii) lagoon and (iv) intertidal–salt marsh. Salinity is recognised as the main driving factor of ostracod communities [23,74] from continental to coastal settings. It was applied to determine the main ostracod ecological groups as follows: (i) freshwater to low brackish; (ii) brackish-marine; (iii) euryhaline and (iv) shallow marine. Ecological attributions of individual taxa are reported in Tables S3 and S4 of the Supplementary Materials. Refined palaeoecological interpretations of

taxa assemblages were obtained by integrating additional papers on the Mediterranean area [75,76].

The cored succession lacks absolute age dating. The chronological framework of the uppermost ~100 m, however, takes advantage from the basin-scale stratigraphic correlations reported in [29]. The lack of unequivocal stratigraphic markers and the complex tectonic setting prevent detailed correlation with published data [30,53] for the lower portion of the core (>100 m core depth).

4. Results

Within the ~205 m-long succession of core 204 S16, nine major facies associations were identified through the integration of sedimentological features, meiofauna content and geotechnical (PP) data (Figure 3). Facies description and interpretation of depositional environments, ranging from alluvial to shallow-marine systems, are reported below. Our interpretations also benefit from the detailed facies characterization of the uppermost 100 m of sediments buried beneath the southern Po coastal plain, reported by [21,77,78].

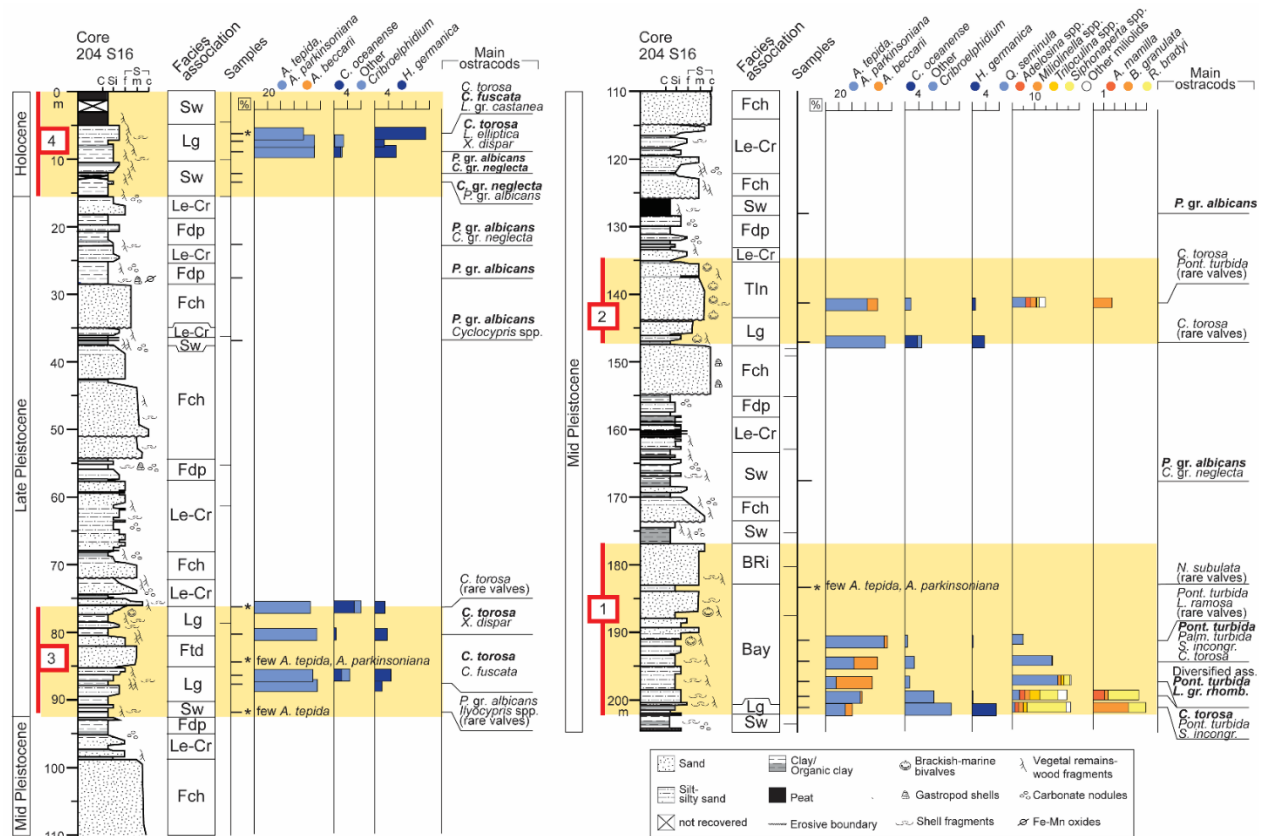


Figure 3. Stratigraphy and facies characterization of the studied core 204 S16. Paralic to marine units rich in meiofauna are highlighted and numbered in stratigraphic order (Units 1–4). Abbreviations of facies associations are explained in text (Section 4). Sedimentological features are reported along with the meiofauna content; samples barren of autochthonous meiofauna are shown on the left. Asterisks mark samples containing less than 100 tests of benthic foraminifers. Relative abundances of main benthic foraminifer taxa are displayed, as well as the vertical distribution of key taxa composing ostracod assemblages (dominant taxa are highlighted in bold). Miliolids and epiphytic species, as *A. mamilla*, *B. granulata* and *R. bradyi*, are not represented in the 0–100 m interval due to their extreme paucity (<1.5%). C: Clay; Si: Silt; S: sand (f: fine, m: medium, c: coarse).

4.1. Fluvial-Channel Facies Association (Fch)

4.1.1. Description

This facies association is recorded at various stratigraphic intervals throughout the cored succession. It is composed of ~3 to 15 m-thick, grey to dark grey sandy bodies (from fine to coarse sand) with a sharp lower boundary. The upper boundary is either sharp or transitional to the overlying muddy deposits. Sedimentary structures are not detected. A fining-upward (FU) grain-size trend culminating in a silty sand-sandy silt interval slightly enriched in decomposed organic matter (OM) is locally recorded. Vegetal remains, wood fragments and few shells or fragments of gastropods commonly occur. The meiofauna is absent. Scattered carbonate nodules typify the silty intervals atop the sandy successions.

4.1.2. Interpretation

The distinct lithological-sedimentological features, including granulometry, thickness, vertical grain-size variations (FU) and the sharp (likely erosional) lower boundary, accompanied by the absence of meiofauna point to a sandy fluvial-channel facies association. The occurrence of vegetal-wood debris and scattered mollusc fragments is a common feature of channel deposits [78]. Atop FU successions, silty intervals with carbonate nodules and organic materials may reflect the gradual abandonment of the channel.

4.2. Levee and Crevasse Facies Association (Le-Cr)

4.2.1. Description

This facies association, encountered at various core intervals, includes m-thick, grey-dark grey sediment bodies composed of: (i) cm to dm alternation of silt-sandy silt and silty sands deposits with the occasional presence of coarser (i.e., fine to medium sands) layers, for a total thickness of ~2–10 m, or (ii) FU or CU (coarsening upward) sand-silt successions, less than 2 m thick. FU successions have sharp lower boundaries. Silty layers locally include carbonate nodules and rootlets. Thin organic-rich layers are common. Mollusc fragments are scattered and the meiofauna is absent.

4.2.2. Interpretation

Lithological-sedimentological features indicate a channel-related depositional environment subject to overflow events and, occasionally, OM accumulation likely favoured by the development of local depressions in proximity of the river axis. Specifically, sand-silt alternations could reflect levee deposits and/or the distal fringes of a crevasse splay, while FU/CU sandy bodies likely correspond with crevasse channels/splays. The occurrence of carbonate nodules and the absence of the meiofauna support this interpretation, pointing to a subaerially exposed environment, characterised by frequent water table variations.

4.3. Floodplain Facies Association (Fdp)

4.3.1. Description

Grey to darkish grey clay-silt deposits of variable thickness (~2–10 m) with carbonate nodules and scattered Fe-Mn oxides characterise this facies association, recorded at various stratigraphic levels along the core. Locally, dm to cm-thick silty sand layers occur as well as sparse vegetal remains, thin OM-enriched layers, mollusc shells (i.e., gastropods) and fragments. PP values are commonly >2 kg/cm² with peaks > 5 kg/cm² especially where muds exhibit abundant carbonate concretions. The meiofauna is generally absent, with the exception of two stratigraphic intervals in the uppermost portion of the core (between ~28–25 m and ~22–21 m core depth), where a quite rich ostracod fauna dominated by *Pseudocandona* ex gr. *albicans* and characterised by the subordinate occurrence of *Candona* ex gr. *neglecta*, *Cyclocypris* spp. and *Ilyocypris* spp. is found. These intervals also show PP values <2 kg/cm².

4.3.2. Interpretation

Based on the dominance of muds and the diffuse presence of pedogenic features, this facies association is interpreted to reflect a low-energy alluvial setting, such as a floodplain, only occasionally affected by overflow events physically recorded by silty sand layers. Well-drained conditions can be associated to the intervals barren of meiofauna and showing high consistency; peaks $>5 \text{ kg/cm}^2$ with abundant carbonate nodules are interpreted as pedogenized horizons/weakly developed palaeosols [79,80]. Lower PP values paralleled by the occurrence of an autochthonous hypohaline ostracod fauna point to a poorly drained floodplain with ephemeral ponds. This interpretation is further supported by the high abundance of ostracods preferring shallow, standing waters, such as *P. ex gr. albicans* [65,81].

4.4. Swamp Facies Association (Sw)

4.4.1. Description

This facies association, encountered at various stratigraphic intervals, is 1–6 m thick and it is typified by two distinct fine-grained lithofacies: (i) dark grey silt-clay deposits with subordinate sandy silts and fine sands forming thin (cm to dm-thick) layers, and (ii) dark peaty clays. The former lithofacies is characterised by very soft deposits typified by low PP values, commonly $<1 \text{ kg/cm}^2$, in the uppermost part of the succession ($<35 \text{ m}$ core depth). PP values increase with depth, as testified by the OM-enriched interval recovered around 90 m (2.7 kg/cm^2). Abundant plant and wood debris, mollusc shells (i.e., gastropods belonging to genera *Planorbis* and *Bithynia*) and fragments are frequently recorded. Few carbonate nodules can occur. Locally, a rich ostracod fauna composed of abundant *P. ex gr. albicans* and abundant to scarce *C. ex gr. neglecta* is found, with the second-level occurrence of *Cyclocypris* spp., *Ilyocypris* ssp. and/or *Darwinula stevensoni*. Very few specimens of *Ammonia tepida* were recorded within one sample collected at $\sim 92 \text{ m}$ core depth. The peaty lithofacies is almost entirely composed of vegetal remains with the occurrence of few mollusc fragments and/or carbonate nodules. Samples are barren or display an ostracod fauna including *P. ex gr. albicans* with subordinate *C. ex gr. neglecta* and *Ilyocypris* spp. This lithofacies typifies the uppermost 5 m of the core, where extremely low (0.2 kg/cm^2) PP values are recorded.

4.4.2. Interpretation

The dominance of a muddy sedimentation paralleled by the accumulation-preservation of abundant vegetal remains, the local occurrence of an autochthonous hypohaline ostracod fauna preferring stagnant waters and low oxygen (mainly *P. ex gr. albicans*; [65,81]) and the generally low consistency point to a paludal environment deprived of any obvious marine influence, such as a swamp. The local record of few tests of the euryhaline *A. tepida* [82] is suggestive of coastal wetlands proximity. The peaty lithofacies likely indicates higher levels of the water table and the development of extensive swampy areas in the plain [83]. Sparse carbonate nodules reflect local groundwater-table fluctuations.

4.5. Lagoon Facies Association (Lg)

4.5.1. Description

This few-m thick (1–5.5 m) facies association, recorded at distinct core depths, is composed of grey-dark grey clayey silt to sandy silt deposits, with local CU trends and abundant mollusc fragments and shells, mainly represented by *Cerastoderma glaucum*. Scattered vegetal remains and decomposed OM occur, as well as cm to dm-thick sandy layers. The PP values vary between $2.8\text{--}2.2 \text{ kg/cm}^2$ at remarkable core depths (between $\sim 90\text{--}86 \text{ m}$ and $\sim 80\text{--}76 \text{ m}$ core depth), but they drop to 0.5 kg/cm^2 between $\sim 11\text{--}5 \text{ m}$ core depth. Samples from this facies association commonly display a quite rich, autochthonous meiofauna composed of both ostracods and benthic foraminifers. The ostracod fauna is dominated by the euryhaline species *Cyprideis torosa*, locally associated with a set of brackish-marine taxa, such as *Cytheromorpha fuscata* (co-dominant with *C. torosa* in one sample), *Loxoconcha elliptica*, *Xestoleberis dispar* and *Leptocythere* species (mainly *L. ex gr.*

castanea). Marine species, mainly represented by *Pontocythere turbida* and *Semicytherura incongruens*, are secondarily recorded within one sample collected at ~201 m core depth. This sample also includes a highly diversified benthic foraminiferal assemblage with abundant *Ammonia tepida* and *Ammonia parkinsoniana* (~30%), known to proliferate in transitional and nearshore environments subject to river discharge [66], and subordinate shallow marine taxa, including *Siphonaperta* spp. (~17.5%), *Ammonia beccarii* (~10.5%) and *Criboelphidium lidoense* (~6%), among others. All the other samples containing foraminifers are almost entirely composed of *A. tepida* and *A. parkinsoniana* (~95–75%), with the second-level occurrence of species typically thriving brackish, semi-protected environments, such as *Haynesina germanica* (~2–15%) and *Criboelphidium oceanense* (<6%) [68–70].

4.5.2. Interpretation

Sedimentological features (e.g., grain-size, thickness) and the particular fossil content, mainly typified by taxa (i.e., *A. tepida*, *A. parkinsoniana*, *C. torosa*, *C. glaucum*) proliferating within Mediterranean coastal basins able to tolerate brackish and schizohaline conditions [82,84], suggest a semi-protected, back-barrier environment, such as a lagoon. Specifically, the secondary species accompanying *C. torosa*, *A. tepida* and *A. parkinsoniana* are indicative of central lagoon conditions with a reduced sea-water exchange (*sensu* [71]). An exception is the sample at ~201 m core depth that records an outer lagoon sub-environment subject to a higher sea-influence, as testified by the more diversified meiofauna including typical shallow marine ostracods and benthic foraminifers [63,82]. The local increase in sand content (i.e., sandy layers; CU trends) likely reflects the occurrence of high-energy events, potentially linked to the activity of sea or river currents in a lagoon.

4.6. Flood-Tidal Delta Facies Association (Ftd)

4.6.1. Description

A ~5 m-thick, grey sand-silty body showing a roughly CU trend and abundant vegetal remains characterises this facies association, exclusively recorded between ~81–86 m core depth. Few mollusc fragments are also encountered. The meiofauna is composed of rare *A. tepida* and *A. parkinsoniana* accompanied by several valves of *C. torosa* and *C. fuscata*, which co-dominate the ostracod fauna. Few poorly preserved tests of *H. germanica* and valves of *Pseudocandona* also occur.

4.6.2. Interpretation

Sedimentological features and meiofauna content suggest a back-barrier (brackish) depositional setting subject to moderate levels of energy at the bottom. The remarkable abundance of the silt fraction and vegetal remains, the CU trend and the occurrence of a mesohaline species (*C. fuscata*; [61,82]) commonly found in association with the euryhaline *C. torosa* within tidal-influenced sub-environments [85,86] point to a flood-tidal delta, likely its distal fringes. This interpretation is consistent with the occurrence of scattered valves of hypohaline ostracods.

4.7. Tidal Inlet Facies Association (TIn)

4.7.1. Description

This facies association, exclusively recorded between ~144–135 m core depth above lagoon deposits, is composed of a m-thick, massive, grey sand body showing a sharp base and a marked FU trend from coarse to silty sands. Atop the succession, thin OM-enriched layers occur; abundant mollusc shells, mainly *C. glaucum* and Pectinidae, typify the entire sandy deposit. A rich, quite diversified foraminiferal assemblage is encountered with abundant *A. tepida* and *A. parkinsoniana* (~60%) accompanied by marine taxa, such as *A. beccarii* (~16%), miliolids (for instance, *Adelosina* spp. and *Miliolinella* spp., ~5% in total) and the epiphytic *Buccella granulata* (~2%), as well as the brackish species *H. germanica* (~1%). Species able to thrive both transitional and shallow marine settings as *Quinqueloculina*

seminula (6%) are also encountered. Among ostracods, few valves of the euryhaline *C. torosa* and shallow-marine *Pontocythere turbida* are recorded.

4.7.2. Interpretation

This facies association is inferred to have been deposited in a high-energy setting under the action of sea currents, as testified by the coarse grain-size and the fossil content typified by the occurrence of marine taxa, such as *A. beccarii*, *B. granulata*, *Pontocythere turbida*. Sedimentological features including thickness, grain-size trend and the sharp lower boundary, interpreted as erosive, integrated with the stratigraphic position and the mixed marine-brackish fauna point to a channel-fill succession developed at the transition between a back-barrier basin and the open coast, possibly a tidal inlet or a major tidal channel [87,88]. A similar foraminiferal assemblage characterises the tidal inlets of the Venice lagoon [64]. The scarcity of ostracod valves is consistent with this interpretation, as high hydrodynamic conditions represent a limiting factor for ostracod communities [74]. The occurrence of organic-rich layers atop the sandy succession points to the deactivation of the inlet.

4.8. Beach Ridge Facies Association (BRi)

4.8.1. Description

A ~6 m-thick sand body composed of grey fine-medium to coarse sands organised into a CU trend characterises this facies association, exclusively encountered between ~183–177 m core depth above a muddy succession including marine molluscs. Scattered vegetal fragments and mollusc fragments are found. Thin (cm-thick) silty layers occur and a coarse-sand, organic-rich interval caps the sandy succession. The meiofauna is absent.

4.8.2. Interpretation

Sedimentological features and the stratigraphic position of this facies association point to a high-energy, coastal environment, such as a beach ridge. The accumulation of OM atop the sandy succession likely reflects the transition to a backshore swale.

4.9. Bay Facies Association (Bay)

4.9.1. Description

This facies association corresponds to a ~18 m-thick grey silt-sand body, showing an overall CU trend with basal silty sands (~201–190 m core depth) passing upward to fine sands (~190–183 m core depth). Mollusc shells (marine bivalves and gastropods), mollusc and echinoderm fragments, vegetal remains and wood debris are commonly encountered. A rich and highly diversified meiofauna typifies the lower silty portion. Among benthic foraminifers, *Ammonia* species, including *A. tepida* and *A. parkinsoniana* (~16–89%) and *A. beccarii* (~2.5–55%), are the dominant taxa with the second-level occurrence of *Q. seminula* (~3–20%) and locally of other miliolids as *Siphonaperta* spp. (<8%), *Triloculina* spp. (<5%), *Adelosina* spp. (<2.5%) and *Miliolinella* spp. (<2%). Few specimens of *Criboelphidium* spp., mainly *C. poeyanum* (<3%) and *C. granosum* (<2%), also occur. Specifically, an overall decreasing-increasing trend of *A. tepida* and *A. parkinsoniana* is paralleled by an opposite trend of *A. beccarii* and, to a lesser extent, of *Q. seminula*. Other miliolids and hyaline epiphytic taxa, including *Asterigerinata mamilla*, *B. granulata* and *Rosalina bradyi*, are almost exclusively recorded within the lowermost interval of the silty succession (~200–195 m core depth), where a diversified marine ostracod fauna is found. Common valves of *Pontocythere turbida* and *Loxoconcha* ex gr. *rhomboidea* are here associated to *Sagmocythere napoliana*, *Palmoconcha turbida*, *Carinocythereis whitei*, *Cytheridea neapolitana* and *Semicytherura* species (mainly *S. incongruens*). Few valves of the brackish-marine *Loxoconcha stellifera*, *Leptocythere bacescoi* and *Leptocythere ramosa* also occur. Upwards (~195–190 m core depth), ostracods show a marked decrease in terms of abundance and taxa, as few valves of *Pontocythere turbida* and *Leptocythere* species are found along with the local appearance of *C. torosa*.

The uppermost sandy portion of this facies association (~190–183 m core depth) is almost barren in meiofauna with the exception of few specimens of *A. tepida* and *A. parkinsoniana* and the nearshore ostracod *Neocytherideis subulata*.

4.9.2. Interpretation

The sedimentological features and the particular meiofauna content, typified by the dominance of shallow-marine taxa with the second-level occurrence of brackish-marine ostracods and benthic foraminifers able to thrive river-influenced settings (*A. tepida*, *A. parkinsoniana* and *Q. seminula*), point to a partially sheltered basin with salinity close to marine values, such as a bay/gulf. The stratigraphic distribution of *Ammonia* species (*A. tepida*, *A. parkinsoniana* versus *A. beccarii*), miliolids and hyaline epiphytic taxa reflects an upward increase in river influence paralleled by a shallowing trend, also highlighted by the sand content. Changes in the ostracod fauna composition (i.e., appearance of *Leptocythere* species and *C. torosa*) and structure (i.e., decrease in species richness and absolute abundance) support this interpretation. The uppermost sandy portion is interpreted to record an approaching shoreline.

5. Discussion

5.1. Core Stratigraphy and Bio-Sedimentary Trends

The integrated stratigraphic analysis and detailed facies characterization of core 204 S16 allow the robust identification of alternating paralic to shallow-marine—alluvial deposits within a significant portion of the Quaternary record (Figures 1 and 3). Four fossiliferous stratigraphic units composed of swamp/lagoon to bay sediments are identified via meiofauna analyses at ~201–177 m; 147–135 m; 92–76 m and 15–0 m core depth (Units 1–4 in Figure 3). Published chronological data and stratigraphic correlations across the study area constrain the two youngest units (Units 3, 4) to the last 125–130 kyrs, whereas Units 1 and 2 can be attributed to the Middle Pleistocene in a general way only [29,37]. These units are sandwiched between sedimentary successions tens of m thick, almost deprived of body fossils and formed by a variety of coarse-grained (fluvial channel) to fine-grained (overbank) alluvial facies associations, locally interrupted by swampy deposits containing at most hypohaline ostracods (mainly *P. ex gr. albicans*, Figure 3).

The lowermost fossiliferous unit (Unit 1), superposed onto swamp deposits barren of meiofauna at the base of the cored succession, displays a remarkable thickness (~25 m) and an obvious deepening-shallowing trend (Figure 3). Outer lagoon muds including both species tolerant to low, variable salinities (e.g., *A. tepida*, *A. parkinsoniana* and *C. torosa*) and marine taxa (e.g., *A. beccarii*, *Siphonaperta* spp., *B. granulata*, *Pontocythere turbida*, *Semicytherura* spp.) are abruptly overlaid by bay deposits, typified by an abundant shallow marine fauna mainly composed of *A. beccarii*, miliolids, *Pontocythere turbida* and *L. ex gr. rhomboidea*. Such an assemblage, characteristic of coarse-grained substrates covered by vegetation, points to water depths <10–15 m [89,90] marking the maximum marine incursion into a coastal embayment. The upward increase of *A. tepida*, *A. parkinsoniana* and the renewed occurrence of the euryhaline *C. torosa* (around 195 m core depth), accompanied by a less diversified and scarce ostracod fauna, record the progressive fill of the bay via coastline progradation, up to the establishment of a beach-ridge complex at the core site (Figure 3). Upwards, a predominantly fine-grained succession of swamp deposits, locally interrupted by 3.5 m-thick fluvial-channel sands, occurs up to ~165 m. The meiofauna suggests here a depositional setting deprived of any significant marine influence pointing to an abrupt seaward migration of facies that culminates with the deposition of sterile overbank sediments, truncated atop by a 7.5 m-thick fluvial channel deposit.

The superposition of ~3 m of lagoonal silts and sands (~147–144 m core depth; Figure 3) marks the lower boundary of the second fossiliferous unit (Unit 2). The brackish assemblage (*A. tepida*, *A. parkinsoniana*, *H. germanica*, *C. oceanense* and *C. torosa*) typical of a central lagoon basin is suddenly replaced by a more diversified, marine-brackish meiofauna found within the overlying tidal inlet sands (Figure 3). Specifically, the decrease

in relative abundance of lagoonal species (*H. germanica*, *C. oceanense*) paralleled by the appearance of miliolids and littoral-sublittoral species, such as *Pontocythere turbida* and *A. beccarii*, records a marine flooding and the approaching of the palaeoshoreline at the core site. Around 135 m core depth, subaerial conditions suddenly re-established as revealed by the development of a ~40 m-thick alluvial succession, mainly composed of overbank deposits and fluvial-channel sands, both barren in meiofauna. However, a 2 m-thick peaty swamp containing freshwater to mesohaline ostracods (i.e., *P. ex gr. albicans*, *C. ex gr. neglecta* and *Ilyocypris* spp.; Figure 3) is found around 127 m core depth, possibly indicating the widespread development of wetlands in the study area. The upper half portion of the alluvial succession includes a ~15 m-thick sandy deposit interpreted as a channel-belt, overlaid by stiff (PP > 5 kg/cm²) and most likely pedogenised levee-crevasse and floodplain sediments. Upwards, around 90 m core depth, the vertical succession of swamp-lagoon muds typifies the lower portion of the third fossiliferous unit (Unit 3) entirely composed of paralic deposits (Figure 3) and chronologically constrained to the Last Interglacial (~130–125 kyrs BP) by [29]. Above swamp deposits containing a scarce hypohaline ostracod fauna and few *A. tepida*, an abundant brackish assemblage (*A. tepida*, *A. parkinsoniana*, *H. germanica*, *C. oceanense*, *C. torosa*, *C. fuscata*) marks the establishment of a central lagoon basin with a moderate sea-water exchange. The record of *C. fuscata* and the superposition of flood-tidal delta silty sands suggest a certain degree of tidal influence in the basin, while the overlying lagoon muds document the re-establishment of low-energy conditions. The decreasing trend in ostracod abundance and richness points to a progressively more confined setting, abruptly followed by alluvial sedimentation around 75 m core depth (Figure 3). Above ~20 m of overbank silt-sand sediments with evidence of pedogenesis atop (PP values 4–5 kg/cm² around 56–54 m core depth), a ~15 m-thick channel-belt body occurs. Upwards, a thin (~2 m) fine-grained succession composed of swamp sediments with hypohaline ostracods and sterile overbank deposits is truncated by a 6 m-thick fluvial channel deposit, overlaid by ~13 m of floodplain muds locally interrupted by overbank silts-sands. The occurrence of a quite rich, hypohaline ostracod fauna along with low PP values (generally <2 kg/cm²) suggest the establishment of poorly drained conditions in the plain (Figure 3).

Upcore, around 15 m core depth, five meters of swamp muds containing abundant valves of freshwater-mesohaline ostracods (i.e., *P. ex gr. albicans* and *C. ex gr. neglecta*) mark the onset of the uppermost paralic unit (Unit 4; Figure 3), chronologically attributed to the Holocene ([29] and references therein). The replacement of hypohaline ostracods by a brackish meiofauna (*A. tepida*, *A. parkinsoniana*, *H. germanica*, *C. torosa*, *L. elliptica* and *X. dispar*) underlines a landward shift of facies, leading to the establishment of a central lagoon basin affected by a moderate sea-water exchange. Within the uppermost portion of the lagoon succession (~7–5 m core depth), a slight increase in the degree of confinement and tidal influence is documented by: (i) the turnover of species accompanying *C. torosa* (i.e., the polyhaline to euhaline *X. dispar* is substituted by the mesohaline *Leptocythere ex gr. castanea* and the oligo-mesohaline *C. fuscata*; [63,73,91]) and (ii) the appearance of the intertidal—salt marsh foraminifer *Trochammina inflata* [92]. This shoaling upward trend culminates with the deposition of 5 m of peaty swamp clays barren in meiofauna and interpreted to reflect freshwater peatlands. These very soft deposits (PP ~ 0.2 kg/cm²) typify the innermost, southern portion of the modern Po delta-coastal plain [93].

5.2. Cyclic Sedimentation during the Middle Pleistocene–Holocene Period: Facies Patterns and Controlling Factors

The cyclic alternation of alluvial and paralic to shallow marine facies associations is a prominent feature of the Quaternary stratigraphy of the long core 204 S16 (Figure 3; Section 5.1). The detailed analysis of the meiofauna associated to the application of ecological groups (Tables S3 and S4) improves the palaeoenvironmental-stratigraphic characterization of the paralic-marine units (Units 1–4), allowing a thorough discussion about facies patterns, age attribution and controlling factors (Figures 3 and 4). Similar to what was observed in other long (>100 m) cores from the study area [27,53], paralic-marine units

are invariably bounded at their base by prominent transgressive surfaces (TS in Figure 4) that mark the onset of major flooding events, reasonably driven by positive glacio-eustatic oscillations in the Milankovitch band (~100 kyrs). The youngest two TSs, recorded at ~90 and 15 m core depth, are correlated to two basin-scale transgressive events recognised by [21,29] and related to the onset of the MIS 5e and Holocene (MIS 1) periods, respectively (Figure 4). However, internal facies architecture of Units 1–4 indicates that the SE Po Plain was affected by different dynamics of marine ingressions during the last hundreds of thousands of years.

The Middle Pleistocene interval (>125–130 kyrs) was typified by more prominent flooding events than the Late Pleistocene-Holocene, as documented by the onset at the core site of coastal depositional environments, thrived by an abundant and diversified marine to brackish-marine meiofauna (Figures 3 and 4). The deepest conditions (<10–15 m water depths) are recorded within the bay deposits of Unit 1 (~200–195 m core depth), where abundant marine taxa (shallow marine foraminifers >35% and marine ostracods >30%; Figure 4) characterise transgressive deposits. As a whole, the retrogradational to progradational stacking pattern of (outer) lagoon-bay-beach ridge deposits is interpreted to reflect the landward migration of the coastline during a phase of RSL rise, followed by progradation during the subsequent highstand. A similar retrogradational pattern of facies, although diagnostic of lower salinity conditions and water depths, is shown by Unit 2, with (central) lagoon deposits overlaid by tidal inlet sands under the forcing of an increasing RSL trend. The superposition of alluvial deposits onto tide-influenced facies prevents further inferences in terms of stratal architecture for Unit 2 (Figure 4).

The lack of absolute ages and biostratigraphic markers hampers any confident chronological (MISs) attribution to Units 1–2 as well as any reliable physical correlations with other cores recovering pre-MIS 5e sediments in the Po Plain, especially in inland areas affected by Quaternary tectonic deformations (e.g., [37,43]). However, sedimentological evidence (i.e., the presence of shallow-marine facies in a relatively inland position) suggests the prominent interglacials MIS 11 and MIS 9 (Figure 4), both exceeding the present sea level [24], as the best candidates for Units 1 and 2, respectively. In particular, the remarkable, long-lasting (~30 kyrs) MIS 11 highstand [94,95] fits well with the establishment of an open-bay environment hosting relatively deep waters (Unit 1; Figures 3 and 4). It is not possible to rule out a MIS 7 age for Unit 2, even though the highest RSL values estimated for the Penultimate Interglacial at most coincide with the present sea level [24,96]. Even more challenging is the chronological attribution of the alluvial successions that abruptly overlies Units 1 and 2. These deposits reasonably formed during glacial periods, when the falling RSL trends forced shoreline regression and led to the widespread establishment of continental environments in the study area. Following [29], the 15 m-thick sand body atop the alluvial succession between Unit 2 and Unit 3 is interpreted to reflect the MIS 6 Po channel-belt. However, the detailed chronostratigraphic reconstruction of the pre-MIS 5e deposits buried beneath the Po Plain still remains an open issue that does not fall into the aims of this study.

The Late Pleistocene-Holocene interval is characterised by two Units (3–4) formed on the landward side of beach-barrier complexes (Figures 3 and 4) and separated by a very thick (~60 m) alluvial succession of last glacial age, including the MIS 4 channel-belt (between ~55–40 m core depth from [29]). Both Units 3 and 4 show a retrogradational to progradational stacking pattern of facies that is interpreted to reflect the rising RSL trends and the subsequent highstands of MIS 5e and MIS 1 ages, respectively. Despite the paucity of marine meiofauna (Figure 4), the characteristic facies associations and their vertical succession (swamp-lagoon-flood tidal delta-lagoon for Unit 3; swamp-lagoon-swamp for Unit 4) suggest a more severe marine ingressions in the plain during the Last Interglacial. This is in accordance with the estimated MIS 5e RSL, which was significantly higher than the modern one (4–9 m above present sea level; [97,98]) and determined a more landward migration of the shoreline in the study area [29].

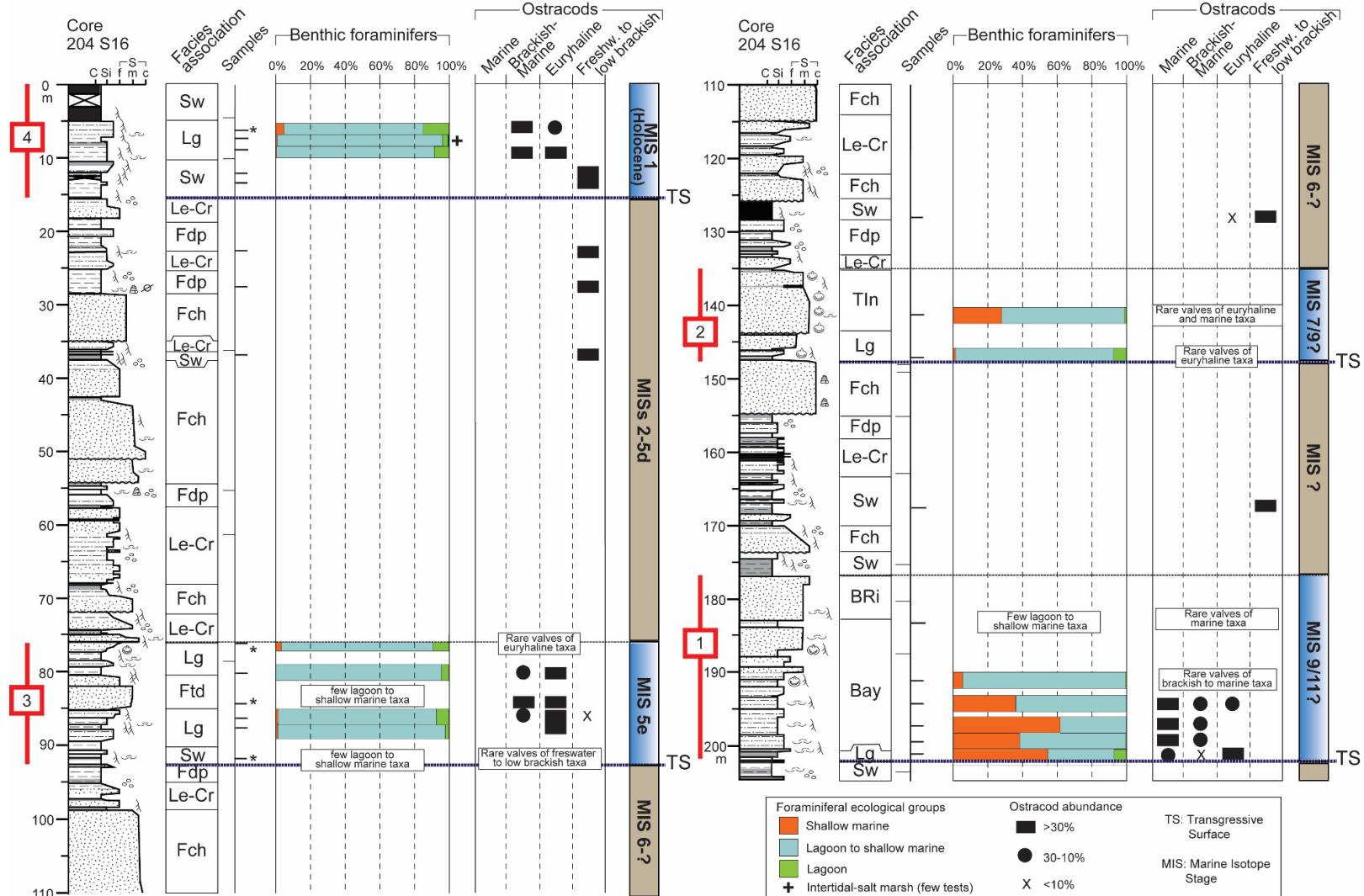


Figure 4. Stratigraphic distribution of benthic foraminifer and ostracod ecological groups along core 204 S16. Boundaries of the Units 1–4 are highlighted. TS: Transgressive Surface. The interpretation in terms of Marine Isotope Stages (MISs) is also reported. See the legend and caption of Figure 3 for lithological information.

Although supporting a predominant glacio-eustatic forcing at the Milankovitch-scale, the cyclic sedimentation patterns of Middle Pleistocene-Holocene age in core 204 S16 display an overall “regressive” pattern that mimics the shallowing-upward trend of the Po Basin fill. Specifically, stratigraphic changes in meiofauna communities progressively track an upward decrease in marine influence within the successive paralic-marine units encountered along the 205 m-long core profile (Units 1–4; Figure 4). Though forcing factors cannot easily be resolved without additional chronological and stratigraphic data and require a full three-dimensional control on facies architecture, the vertical stacking pattern of facies illustrated in this study could reasonably suggest a combined control by Quaternary RSL dynamics and the tectonic evolution of the basin.

6. Conclusions

The vertical stacking pattern of facies associations recorded along core 204 S16, ~205 m long, coupled with stratigraphic trends in meiofauna palaeocommunities, provide new insights about the Middle Pleistocene-Holocene evolution dynamics of the rapidly subsiding Po Plain through the overcoming of a repeated sequence of Milankovitch-scale (~100 kyrs) glacial-interglacial cycles.

We summarise the major results as follows:

- The long-term bio-sedimentary record of the Po coastal plain reconstructed over a significant portion (last ~300–400 kyrs) of the post-Middle Pleistocene Revolution interval, confirms the pivotal role of glacio-eustatic oscillations on depositional and environmental dynamics.
- A cyclic sedimentation is highlighted by the alternation of tens m-thick alluvial deposits and paralic to shallow-marine units (Units 1–4). These latter are invariably underlined by prominent transgressive surfaces that mark major flooding events in the plain and the abrupt landward shift of depositional environments. Based on previous stratigraphic reconstructions, the two youngest units (Units 3 and 4) are attributed to the Last Interglacial and to the Holocene, respectively. Therefore, Unit 2 and Unit 1 are chronologically constrained to the Middle Pleistocene.
- The strategic position of core 204 S16, well behind the Holocene maximum marine ingression, and the application of an integrated methodology involving meiofauna ecological groups allow reconstructing distinct stratigraphic patterns for the Middle Pleistocene (lowermost ~100 m) and Late Pleistocene-Holocene (uppermost ~100 m) intervals. The former includes coastal to shallow-marine deposits (Units 1, 2), while the latter is typified by the occurrence of back-barrier sediments (Units 3 and 4).
- The lower portions of Units 1–4 invariably exhibit a retrogradational pattern of facies that tracks the transgression under the forcing of rising sea levels; an evident progradational pattern characterises the upper portions of Units 1, 2 and 4, likely reflecting RSL highstand conditions.
- The meiofauna tracks the deepest conditions within the oldest Unit 1; the development of a bay, reasonably in response to a prominent rise in RSL, is attributable to MIS 11 or MIS 9.
- An overall regressive trend is documented within the Middle Pleistocene-Holocene succession of the SE Po Plain, as progressively fewer marine conditions established during interglacials through time, reasonably in response to a complex interaction between glacio-eustatic dynamics and tectonic evolution of the Po Basin over hundreds of thousands of years.

Supplementary Materials: The following are available online at <https://www.mdpi.com/article/10.3390/geosciences11100401/s1>, Table S1: Benthic foraminifer counts. Samples barren of benthic foraminifers are not shown. Colors refer to the ecological groups (listed in Table S3): orange: shallow marine; light blue: lagoon to shallow marine; light green: lagoon; dark green: intertidal–salt marsh. Table S2: Ostracod semi-quantitative data. Samples barren of ostracods or containing <20 valves are not shown. Colors refer to the ecological groups listed in Table S4: orange: marine; dark blue: brackish-marine; light blue: euryhaline; green: freshwater to low brackish. Table S3:

Benthic foraminiferal ecological groups and assigned taxa, in accordance with distributions reported in [62,64,66,70–72,99]. Table S4: Ostracod ecological groups and assigned taxa based on salinity preferences, in accordance with [73] and references therein.

Author Contributions: Conceptualization, V.R., A.A., G.B., S.C.V. and B.C.; methodology, M.G., G.B., S.C.V. and V.R.; writing—original draft preparation, V.R.; writing—review and editing, A.A., G.B., B.C. and S.C.V.; figure preparation, G.B., M.G., B.C. and V.R. All the authors contributed to the discussion (V.R., A.A., G.B., S.C.V., M.G. and B.C.). All authors have read and agreed to the published version of the manuscript.

Funding: This research received no external funding.

Institutional Review Board Statement: Not applicable.

Informed Consent Statement: Not applicable.

Data Availability Statement: The data presented in this study are available at Supplementary Material.

Acknowledgments: We warmly thank the handling editor Emanuela Mattioli and two anonymous reviewers for their constructive comments and suggestions. Regione Emilia-Romagna—RER—Geological, Seismic, and Soil Survey is acknowledged for providing core material. We are indebted to Irene Albino for technical support in samples preparation.

Conflicts of Interest: The authors declare no conflict of interest.

References

1. Anthony, E.J.; Marriner, N.; Morhange, C. Human Influence and the Changing Geomorphology of Mediterranean Deltas and Coasts over the Last 6000 Years: From Progradation to Destruction Phase? *Earth-Sci. Rev.* **2014**, *139*, 336–361. [\[CrossRef\]](#)
2. Peeters, J.; Busschers, F.S.; Stouthamer, E. Fluvial Evolution of the Rhine during the Last Interglacial-Glacial Cycle in the Southern North Sea Basin: A Review and Look Forward. *Quat. Int.* **2015**, *357*, 176–188. [\[CrossRef\]](#)
3. Peeters, J.; Busschers, F.S.; Stouthamer, E.; Bosch, J.H.A.; Van den Berg, M.W.; Wallinga, J.; Versendaal, A.J.; Bunnik, F.P.M.; Middelkoop, H. Sedimentary Architecture and Chronostratigraphy of a Late Quaternary Incised-Valley Fill: A Case Study of the Late Middle and Late Pleistocene Rhine System in the Netherlands. *Quat. Sci. Rev.* **2016**, *131*, 211–236. [\[CrossRef\]](#)
4. Sarti, G.; Rossi, V.; Amorosi, A.; Bini, M.; Giacomelli, S.; Pappalardo, M.; Ribecai, C.; Ribolini, A.; Sammartino, I. Climatic Signature of Two Mid-Late Holocene Fluvial Incisions Formed under Sea-Level Highstand Conditions (Pisa Coastal Plain, NW Tuscany, Italy). *Palaeogeogr. Palaeoclimatol. Palaeoecol.* **2015**, *424*, 183–195. [\[CrossRef\]](#)
5. Amorosi, A.; Maselli, V.; Trincardi, F. Onshore to Offshore Anatomy of a Late Quaternary Source-to-Sink System (Po Plain-Adriatic Sea, Italy). *Earth-Sci. Rev.* **2016**, *153*, 212–237. [\[CrossRef\]](#)
6. Antonioli, F.; Anzidei, M.; Amorosi, A.; Lo Presti, V.; Mastronuzzi, G.; Deiana, G.; De Falco, G.; Fontana, A.; Fontolan, G.; Lisco, S.; et al. Sea-Level Rise and Potential Drowning of the Italian Coastal Plains: Flooding Risk Scenarios for 2100. *Quat. Sci. Rev.* **2017**, *158*, 29–43. [\[CrossRef\]](#)
7. Alizad, K.; Hagen, S.C.; Medeiros, S.C.; Bilskie, M.V.; Morris, J.T.; Balthis, L.; Buckel, C.A. Dynamic Responses and Implications to Coastal Wetlands and the Surrounding Regions under Sea Level Rise. *PLoS ONE* **2018**, *13*, 1–27. [\[CrossRef\]](#)
8. Anderson, C.C.; Renaud, F.G.; Hagenlocher, M.; Day, J.W. Assessing Multi-Hazard Vulnerability and Dynamic Coastal Flood Risk in the Mississippi Delta: The Global Delta Risk Index as a Social-Ecological Systems Approach. *Water* **2021**, *13*, 577. [\[CrossRef\]](#)
9. Grotoli, E.; Bertoni, D.; Ciavola, P. Short- and Medium-Term Response to Storms on Three Mediterranean Coarse-Grained Beaches. *Geomorphology* **2017**, *295*, 738–748. [\[CrossRef\]](#)
10. Luppichini, M.; Bini, M.; Paterni, M.; Berton, A.; Merlino, S. A New Beach Topography-Based Method for Shoreline Identification. *Water* **2020**, *12*, 3110. [\[CrossRef\]](#)
11. Melet, A.; Teatini, P.; Le Cozannet, G.; Jamet, C.; Conversi, A.; Benveniste, J.; Almar, R. *Earth Observations for Monitoring Marine Coastal Hazards and Their Drivers*; Springer: Berlin/Heidelberg, Germany, 2020; Volume 41, ISBN 0123456789.
12. Salvi, G.; Acquavita, A.; Celio, M.; Ciriaco, S.; Cirilli, S.; Fernetti, M.; Pugliese, N. Ostracod Fauna: Eyewitness to Fifty Years of Anthropogenic Impact in the Gulf of Trieste. A Potential Key to the Future Evolution of Urban Ecosystems. *Sustainability* **2020**, *12*, 6954. [\[CrossRef\]](#)
13. Leorri, E.; Cearreta, A.; Irabien, M.J.; Yusta, I. Geochemical and Microfaunal Proxies to Assess Environmental Quality Conditions during the Recovery Process of a Heavily Polluted Estuary: The Bilbao Estuary Case (N. Spain). *Sci. Total Environ.* **2008**, *396*, 12–27. [\[CrossRef\]](#)
14. Francescangeli, F.; Armynot du Chatelet, E.; Billon, G.; Trentesaux, A.; Bouchet, V.M.P. Palaeo-Ecological Quality Status Based on Foraminifera of Boulogne-Sur-Mer Harbour (Pas-de-Calais, Northeastern France) over the Last 200 Years. *Mar. Environ. Res.* **2016**, *117*, 32–43. [\[CrossRef\]](#) [\[PubMed\]](#)

15. Barbieri, G.; Rossi, V.; Ghosh, A.; Vaiani, S.C. Conservation Paleobiology as a Tool to Define Reference Conditions in Naturally Stressed Transitional Settings: Micropaleontological Insights from the Holocene of the Po Coastal Plain (Italy). *Water* **2020**, *12*, 3420. [[CrossRef](#)]
16. Pasquetti, F.; Vaselli, O.; Zanchetta, G.; Nisi, B.; Lezzerini, M.; Bini, M.; Mele, D. Sedimentological, Mineralogical and Geochemical Features of Late Quaternary Sediment Profiles from the Southern Tuscany Hg Mercury District (Italy): Evidence for the Presence of Pre-Industrial Mercury and Arsenic Concentrations. *Water* **2020**, *12*, 1998. [[CrossRef](#)]
17. Bouchet, V.M.P.; Frontalini, F.; Francescangeli, F.; Sauriau, P.G.; Geslin, E.; Martins, M.V.A.; Almogi-Labin, A.; Avnaim-Katav, S.; Di Bella, L.; Cearreta, A.; et al. Indicative Value of Benthic Foraminifera for Biomonitoring: Assignment to Ecological Groups of Sensitivity to Total Organic Carbon of Species from European Intertidal Areas and Transitional Waters. *Mar. Pollut. Bull.* **2021**, *164*, 112071. [[CrossRef](#)] [[PubMed](#)]
18. Schuerch, M.; Spencer, T.; Temmerman, S.; Kirwan, M.L.; Wolff, C.; Lincke, D.; McOwen, C.J.; Pickering, M.D.; Reef, R.; Vafeidis, A.T.; et al. Future Response of Global Coastal Wetlands to Sea-Level Rise. *Nature* **2018**, *561*, 231–234. [[CrossRef](#)] [[PubMed](#)]
19. Milli, S.; Mancini, M.; Moscatelli, M.; Stigliano, F.; Marini, M.; Cavinato, G.P. From River to Shelf, Anatomy of a High-Frequency Depositional Sequence: The Late Pleistocene to Holocene Tiber Depositional Sequence. *Sedimentology* **2016**, *63*, 1886–1928. [[CrossRef](#)]
20. Melis, R.T.; Di Rita, F.; French, C.; Marriner, N.; Montis, F.; Serreli, G.; Sulas, F.; Vacchi, M. 8000 years of Coastal Changes on a Western Mediterranean Island: A Multiproxy Approach from the Posada Plain of Sardinia. *Mar. Geol.* **2018**, *403*, 93–108. [[CrossRef](#)]
21. Amorosi, A.; Bruno, L.; Campo, B.; Morelli, A.; Rossi, V.; Scarponi, D.; Hong, W.; Bohacs, K.M.; Drexler, T.M. Global Sea-Level Control on Local Parasequence Architecture from the Holocene Record of the Po Plain, Italy. *Mar. Pet. Geol.* **2017**, *87*, 99–111. [[CrossRef](#)]
22. Ronchi, L.; Fontana, A.; Cohen, K.M.; Stouthamer, E. Late Quaternary Landscape Evolution of the Buried Incised Valley of Concordia Sagittaria (Tagliamento River, NE Italy): A Reconstruction of Incision and Transgression. *Geomorphology* **2021**, *373*, 107509. [[CrossRef](#)]
23. Rossi, V.; Barbieri, G.; Vaiani, S.C.; Cacciari, M.; Bruno, L.; Campo, B.; Marchesini, M.; Marvelli, S.; Amorosi, A. Millennial-Scale Shifts in Microtidal Ecosystems during the Holocene: Dynamics and Drivers of Change from the Po Plain Coastal Record (NE Italy). *J. Quat. Sci.* **2021**, *36*, 961–979. [[CrossRef](#)]
24. Waelbroeck, C.; Labeyrie, L.; Michel, E.; Duplessy, J.C.; McManus, J.F.; Lambeck, K.; Balbon, E.; Labracherie, M. Sea-Level and Deep Water Temperature Changes Derived from Benthic Foraminifera Isotopic Records. *Quat. Sci. Rev.* **2002**, *21*, 295–305. [[CrossRef](#)]
25. Antonioli, F.; Dai Pra, G.; Hearty, P.J. I Sedimenti Quaternari Nella Fascia Costiera Della Piana Di Fondi (Lazio Meridionale). *Boll. Soc. Geol. Ital. (Ital. J. Geosci.)* **1988**, *107*, 491–501.
26. Romano, P.; Santo, A.; Voltaggio, M. L'evoluzione Geomorfologica Della Pianura Del Fiume Volturno (Campania) Durante Il Tardo Quaternario (Pleistocene Medio-Superiore—Olocene). *Alp. Mediterr. Quat.* **1994**, *7*, 41–55.
27. Amorosi, A.; Colalongo, M.L.; Fiorini, F.; Fusco, F.; Pasini, G.; Vaiani, S.C.; Sarti, G. Palaeogeographic and Palaeoclimatic Evolution of the Po Plain from 150-Ky Core Records. *Glob. Planet. Chang.* **2004**, *40*, 55–78. [[CrossRef](#)]
28. Carboni, M.G.; Bergamin, L.; Di Bella, L.; Esu, D.; Cerone, E.P.; Antonioli, F.; Verrubbi, V. Palaeoenvironmental Reconstruction of Late Quaternary Foraminifera and Molluscs from the ENEA Borehole (Versilian Plain, Tuscany, Italy). *Quat. Res.* **2010**, *74*, 265–276. [[CrossRef](#)]
29. Campo, B.; Bruno, L.; Amorosi, A. Basin-Scale Stratigraphic Correlation of Late Pleistocene-Holocene (MIS 5e-MIS 1) Strata across the Rapidly Subsiding Po Basin (Northern Italy). *Quat. Sci. Rev.* **2020**, *237*. [[CrossRef](#)]
30. Amorosi, A.; Colalongo, M.L.; Fusco, F.; Pasini, G.; Fiorini, F. Glacio-Eustatic Control of Continental-Shallow Marine Cyclicity from Late Quaternary Deposits of the Southeastern Po Plain, Northern Italy. *Quat. Res.* **1999**, *52*, 1–13. [[CrossRef](#)]
31. Amorosi, A.; Forlani, L.; Fusco, F.; Severi, P. Cyclic Patterns of Facies and Pollen Associations from Late Quaternary Deposits in the Subsurface of Bologna. *GeoActa* **2001**, *1*, 83–94.
32. Kent, D.V.; Rio, D.; Massari, F.; Kukla, G.; Lanci, L. Emergence of Venice during the Pleistocene. *Quat. Sci. Rev.* **2002**, *21*, 1719–1727. [[CrossRef](#)]
33. Bossio, A.; Ciampo, G.; Dall'Antonia, B. Quaternary Environmental Evolution of the Venice Area Based upon Ostracod Assemblages. *Boll. Della Soc. Paleontol. Ital.* **2004**, *43*, 113–122.
34. Massari, F.; Rio, D.; Serandrei Barbero, R.; Asioli, A.; Capraro, L.; Fornaciari, E.; Vergerio, P.P. The Environment of Venice Area in the Past Two Million Years. *Palaeogeogr. Palaeoclimatol. Palaeoecol.* **2004**, *202*, 273–308. [[CrossRef](#)]
35. Carminati, E.; Di Donato, G. Separating Natural and Anthropogenic Vertical Movements in Fast Subsiding Areas: The Po Plain (N. Italy) Case. *Geophys. Res. Lett.* **1999**, *26*, 2291–2294. [[CrossRef](#)]
36. Ghielmi, M.; Minervini, M.; Nini, C.; Rogledi, S.; Rossi, M. Late Miocene-Middle Pleistocene Sequences in the Po Plain—Northern Adriatic Sea (Italy): The Stratigraphic Record of Modification Phases Affecting a Complex Foreland Basin. *Mar. Pet. Geol.* **2013**, *42*, 50–81. [[CrossRef](#)]
37. Amorosi, A.; Bruno, L.; Campo, B.; Costagli, B.; Hong, W.; Picotti, V.; Vaiani, S.C. Deformation Patterns of Upper Quaternary Strata and Their Relation to Active Tectonics, Po Basin, Italy. *Sedimentology* **2021**, *68*, 402–424. [[CrossRef](#)]

38. Lisiecki, L.E.; Raymo, M.E. A Pliocene-Pleistocene Stack of 57 Globally Distributed Benthic δ 18O Records. *Paleoceanography* **2005**, *20*, 1–17. [[CrossRef](#)]
39. Burrato, P.; Ciucci, F.; Valensise, G. An Inventory of River Anomalies in the Po Plain, Northern Italy: Evidence for Active Blind Thrust Faulting. *Ann. Geophys.* **2003**, *46*, 865–882.
40. Bondesan, M.; Favero, V.; Viñals, M.J. New Evidence on the Evolution of the Po-Delta Coastal Plain during the Holocene. *Quat. Int.* **1995**, *29–30*, 105–110. [[CrossRef](#)]
41. Correggiari, A.; Cattaneo, A.; Trincardi, F. Depositional Patterns in the Late Holocene Po Delta System. *SEPM Spec. Publ.* **2005**, *83*, 365–392. [[CrossRef](#)]
42. Carminati, E.; Doglioni, C. Alps vs. Apennines: The Paradigm of a Tectonically Asymmetric Earth. *Earth-Sci. Rev.* **2012**, *112*, 67–96. [[CrossRef](#)]
43. Pieri, M.; Groppi, G. Subsurface Geological Structure of the Po Plain. *Italy Publ.* **1981**, *441*, 1–11.
44. Boccaletti, M.; Corti, G.; Martelli, L. Recent and Active Tectonics of the External Zone of the Northern Apennines (Italy). *Int. J. Earth Sci.* **2011**, *100*, 1331–1348. [[CrossRef](#)]
45. Carminati, E.; Doglioni, C.; Scrocca, D. Apennines Subduction-Related Subsidence of Venice (Italy). *Geophys. Res. Lett.* **2003**, *30*, 1–4. [[CrossRef](#)]
46. Bruno, L.; Campo, B.; Costagli, B.; Stouthamer, E.; Teatini, P.; Zoccarato, C.; Amorosi, A. Factors Controlling Natural Subsidence in the Po Plain. *Proc. Int. Assoc. Hydrol. Sci.* **2020**, *382*, 285–290. [[CrossRef](#)]
47. Amadori, C.; Toscani, G.; Di Giulio, A.; Maesano, F.E.; D’Ambrogio, C.; Ghielmi, M.; Fantoni, R. From Cylindrical to Non-Cylindrical Foreland Basin: Pliocene–Pleistocene Evolution of the Po Plain–Northern Adriatic Basin (Italy). *Basin Res.* **2019**, *31*, 991–1015. [[CrossRef](#)]
48. Mitchum, J.R.M.; Vail, P.R.; III, T.S. Seismic stratigraphy and global changes of sealevel, Part 2: The depositional sequence as a basic unit for stratigraphic analysis. In *American Association of Petroleum Geologists Memoir 26*; Payton, C.E., Ed.; American Association of Petroleum Geologists: Tulsa, OR, USA, 1977; pp. 53–62.
49. Emilia-Romagna, R. *ENI-AGIP Riserve Idriche Sotterranee Della Regione Emilia-Romagna*; S.EL.CA: Firenze, Italy, 1998.
50. Dondi, L.; Mostardini, F.; Rizzini, A. Evoluzione sedimentaria e paleogeografia nella Pianura Padana. In *Guida alla Geologia del Margine Appenninico-Padano*; Cremonini, G., Ricci Lucchi, F., Eds.; IBS: Hong Kong, China, 1982; pp. 47–58.
51. Ghielmi, M.; Minervini, M.; Nini, C.; Rogledi, S.; Rossi, M.; Vignolo, A. Sedimentary and Tectonic Evolution in the Eastern Po-Plain and Northern Adriatic Sea Area from Messinian to Middle Pleistocene (Italy). *Rend. Lincei* **2010**, *21*, 131–166. [[CrossRef](#)]
52. Amorosi, A.; Colalongo, M.L. The linkage between alluvial and coeval nearshoremarine succession: Evidence from the late Quaternary Record of the Po River Plain, Italy. In *Fluvial Sedimentology VII. IAS Special Publication*; Blum, M.D., Marriott, S., Leclair, S.F., Eds.; Wiley Online: Oxford, UK, 2005; pp. 257–275.
53. Amorosi, A.; Colalongo, M.L.; Dinelli, E.; Lucchini, F.; Vaiani, S.C. Cyclic Variations in Sediment Provenance from Late Pleistocene Deposits of the Eastern Po Plain, Italy. *Spec. Pap. Geol. Soc. Am.* **2007**, *420*, 13–24. [[CrossRef](#)]
54. Amorosi, A.; Pavese, M.; Ricci Lucchi, M.; Sarti, G.; Piccin, A. Climatic Signature of Cyclic Fluvial Architecture from the Quaternary of the Central Po Plain, Italy. *Sediment. Geol.* **2008**, *209*, 58–68. [[CrossRef](#)]
55. Bondesan, M.; Cibir, U.; Colalongo, M.L.; Pugliese, N.; Stefani, M.; Tsakiridis, E.; Vaiani, S.C.; Vincenzi, S. Benthic Communities and Sedimentary Facies Recording Late Quaternary Environmental Fluctuations in a Po Delta Subsurface Succession (Northern Italy). In *Proceedings of the Second and Third Italian Meeting of Environmental Micropaleontology*, Urbino, Italy, 4–6 June 2006; Coccioni, R., Lirer, F., Marsili, A., Eds.; The Grzybowski Foundation Special Publication 11: Krakov, Poland, 2006; pp. 21–31.
56. Carta Geologica d’Italia Scala 1:50,000. Available online: <https://www.isprambiente.gov.it/Media/carg/emilia.html> (accessed on 14 August 2021).
57. Emilia-Romagna Geological, Seismic and Soil Survey, Geological Cartography Webgis. Available online: Mappegis.regione.emilia-romagna.it/gstatico/documenti/Masterlog/204080P517X.pdf (accessed on 14 August 2021).
58. Amorosi, A.; Dinelli, E.; Rossi, V.; Vaiani, S.C.; Sacchetto, M. Late Quaternary Palaeoenvironmental Evolution of the Adriatic Coastal Plain and the Onset of Po River Delta. *Palaeogeogr. Palaeoclimatol. Palaeoecol.* **2008**, *268*, 80–90. [[CrossRef](#)]
59. Ellis, B.F.; Messina, A.R. *Catalogue of Foraminifera*; Micropaleontology Press: New York, NY, USA, 1940.
60. Ellis, B.F.; Messina, A.R. *Catalogue of Ostracoda*; The American Museum of Natural History Special Publications: New York, NY, USA, 1952.
61. Bonaduce, G.; Ciampo, G.; Masoli, M. *Distribution of Ostracoda in the Adriatic Sea*; Olschki, L.S., Ed.; Pubblicazioni della Stazione Zoologica di Napoli; The Micropaleontology Project, Inc.: Napoli, Italy, 1975; Volume 40.
62. Jorissen, F.J. *Benthic Foraminifera from the Adriatic Sea; Principles of Phenotypic Variation*; Utrecht Micropaleontological Bulletins: Utrecht, The Netherlands, 1988; Volume 37.
63. Athersuch, J.; Horne, D.J.; Whittaker, J.E. *Marine and Brackish Water Ostracods*; Kermack, D.M., Barnes, R.S.K., Eds.; Synopses of the British Fauna (New Series) 43 Brill, E.J.: Leiden, The Netherlands, 1989.
64. Albani, A.D.; Serandrei Barbero, R. I Foraminiferi Della Laguna e Del Golfo Di Venezia. *Mem. Di Sci. Geol.* **1990**, *42*, 271–341.
65. Henderson, P.A. *Freshwater Ostracods*; Kermack, D.M., Barnes, R.S.K., Eds.; Synopses of the British Fauna (New Series) 42 Brill, E.J.: Leiden, The Netherlands, 1990.
66. Sgarrella, F.; Moncharmont Zei, M. Benthic Foraminifera of the Gulf of Naples (Italy): Systematics and Autoecology. *Boll. Della Soc. Paleontol. Ital.* **1993**, *32*, 145–264.

67. Mazzini, I.; Anadon, P.; Barbieri, M.; Castorina, F.; Ferreli, L.; Gliozzi, E.; Mola, M.; Vittori, E. Late Quaternary Sea-Level Changes along the Tyrrhenian Coast near Orbetello (Tuscany, Central Italy): Palaeoenvironmental Reconstruction Using Ostracods. *Mar. Micropaleontol.* **1999**, *37*, 289–311. [\[CrossRef\]](#)
68. Fiorini, F.; Vaiani, S.C. Benthic Foraminifers and Transgressive-Regressive Cycles in the Late Quaternary Subsurface Sediments of the Po Plain near Ravenna (Northern Italy). *Boll. Della Soc. Paleontol. Ital.* **2001**, *40*, 357–403.
69. Barbieri, G.; Vaiani, S.C. Benthic Foraminifera or Ostracoda? Comparing the Accuracy of Palaeoenvironmental Indicators from a Pleistocene Lagoon of the Romagna Coastal Plain (Italy). *J. Micropaleontol.* **2018**, *37*, 203–230. [\[CrossRef\]](#)
70. Coccioni, R. Benthic foraminifera as bioindicators of heavy metal pollution—A case study from the Goro Lagoon (Italy). In *Environmental Micropaleontology: The Application of Microfossils to Environmental Geology*; Martin, R.E., Ed.; Kluwer Academic/Plenum Publishers: New York, NY, USA, 2000; pp. 71–103.
71. Debenay, J.P.; Guillou, J.J. Ecological Transitions Indicated by Foraminiferal Assemblages in Paralic Environments. *Estuaries* **2002**, *25*, 1107–1120. [\[CrossRef\]](#)
72. Melis, R.; Covelli, S. Distribution and Morphological Abnormalities of Recent Foraminifera in the Marano and Grado Lagoon (North Adriatic Sea, Italy). *Mediterr. Mar. Sci.* **2013**, *14*, 432–450. [\[CrossRef\]](#)
73. Mazzini, I.; Rossi, V.; Da Prato, S.; Ruscito, V. Ostracods in archaeological sites along the Mediterranean coastlines: Three case studies from the Italian peninsula. In *The Archaeological and Forensic Applications of Microfossils: A Deeper Understanding of Human History*; Geological Society of London: London, UK, 2017; pp. 121–142.
74. Frenzel, P.; Boomer, I. The Use of Ostracods from Marginal Marine, Brackish Waters as Bioindicators of Modern and Quaternary Environmental Change. *Palaeogeogr. Palaeoclimatol. Palaeoecol.* **2005**, *225*, 68–92. [\[CrossRef\]](#)
75. Aiello, G.; Amato, V.; Barra, D.; Caporaso, L.; Caruso, T.; Giaccio, B.; Parisi, R.; Rossi, A. Late Quaternary Benthic Foraminiferal and Ostracod Response to Palaeoenvironmental Changes in a Mediterranean Coastal Area, Port of Salerno, Tyrrhenian Sea. *Reg. Stud. Mar. Sci.* **2020**, *40*, 101498. [\[CrossRef\]](#)
76. D'Orefice, M.; Bellotti, P.; Bertini, A.; Calderoni, G.; Neri, P.C.; Di Bella, L.; Fiorenza, D.; Foresi, L.M.; Louvari, M.A.; Rainone, L.; et al. Holocene Evolution of the Burano Paleo-Lagoon (Southern Tuscany, Italy). *Water* **2020**, *12*, 1007. [\[CrossRef\]](#)
77. Bruno, L.; Bohacs, K.M.; Campo, B.; Drexler, T.M.; Rossi, V.; Sammartino, I.; Scarponi, D.; Hong, W.; Amorosi, A. Early Holocene Transgressive Palaeogeography in the Po Coastal Plain (Northern Italy). *Sedimentology* **2017**, *64*, 1792–1816. [\[CrossRef\]](#)
78. Campo, B.; Amorosi, A.; Vaiani, S.C. Sequence Stratigraphy and Late Quaternary Palaeoenvironmental Evolution of the Northern Adriatic Coastal Plain (Italy). *Palaeogeogr. Palaeoclimatol. Palaeoecol.* **2017**, *466*, 265–278. [\[CrossRef\]](#)
79. Amorosi, A.; Bruno, L.; Campo, B.; Morelli, A. The Value of Pocket Penetration Tests for the High-Resolution Palaeosol Stratigraphy of Late Quaternary Deposits. *Geol. J.* **2015**, *50*, 670–682. [\[CrossRef\]](#)
80. Amorosi, A.; Bruno, L.; Cleveland, D.M.; Morelli, A.; Hong, W. Paleosols and Associated Channel-Belt Sand Bodies from a Continuously Subsiding Late Quaternary System (Po Basin, Italy): New Insights into Continental Sequence Stratigraphy. *Bull. Geol. Soc. Am.* **2017**, *129*, 449–463. [\[CrossRef\]](#)
81. Meisch, C. *Freshwater Ostracoda of Western and Central Europe*; Süßwasserfauna von Mitteleuropa; Spektrum Akademischer Verlag: Heidelberg/Berlin, Germany, 2000; Volume 3.
82. Murray, J.W. *Ecology and Applications of Benthic Foraminifera*; Cambridge University Press: Cambridge, UK, 2006.
83. Amorosi, A.; Bruno, L.; Cacciari, M.; Campo, B.; Rossi, V. Tracing Marine Flooding Surface Equivalents across Freshwater Peats and Other Wetland Deposits by Integrated Sedimentological and Pollen Data. *Int. J. Coal Geol.* **2021**, *246*, 103830. [\[CrossRef\]](#)
84. Pint, A.; Frenzel, P. Ostracod Fauna Associated with *Cyprideis torosa*—An Overview. *J. Micropaleontol.* **2017**, *36*, 113–119. [\[CrossRef\]](#)
85. Tibert, N.E.; Walker, L.J.; Patterson, W.P.; Hubeny, J.B.; Jones, E.; Cooper, O.R. A Centennial Record of Paleosalinity Change in the Tidal Reaches of the Potomac and Rappahannock Rivers, Tributaries to Chesapeake Bay. *Va. J. Sci.* **2012**, *63*, 111–128.
86. Horne, D.J.; Benardout, G.; Whittaker, J.E. *Cyprideis torosa* (Jones, 1850) in Its Type Area and Stratigraphical Context: Potential for Mapping the Freshwater/Estuarine Boundaries of the Thames–Medway River System in the MIS 9 and MIS 11 Interglacials. *J. Micropaleontol.* **2017**, *36*, 127–135. [\[CrossRef\]](#)
87. FitzGerald, D.; Buynevich, I.; Hein, C. Morphodynamics and Facies Architecture of Tidal Inlets and Tidal Deltas. In *Principles of Tidal Sedimentology*; Davis, R.A., Dalrymple, R.W., Eds.; Springer: Berlin/Heidelberg, Germany, 2011; ISSN 9789400701236.
88. Zecchin, M.; Tosi, L.; Caffau, M.; Baradello, L.; Donnici, S. Sequence Stratigraphic Significance of Tidal Channel Systems in a Shallow Lagoon (Venice, Italy). *Holocene* **2014**, *24*, 646–658. [\[CrossRef\]](#)
89. Aiello, G.; Barra, D.; Coppa, M.G.; Valente, A.; Zeni, F. Recent Infralittoral Foraminifera and Ostracoda from the Porto Cesareo Lagoon (Ionian Sea, Mediterranean). *Boll. Della Soc. Paleontol. Ital.* **2006**, *45*, 1–14.
90. Tsourou, T. Composition and Distribution of Recent Marine Ostracod Assemblages in the Bottom Sediments of Central Aegean Sea (SE Andros Island, Greece). *Int. Rev. Hydrobiol.* **2012**, *97*, 276–300. [\[CrossRef\]](#)
91. Frenzel, P.; Keyser, D.; Viehberg, F.A. An Illustrated Key and (Palaeo)Ecological Primer for Postglacial to Recent Ostracoda (Crustacea) of the Baltic Sea. *Boreas* **2010**, *39*, 567–575. [\[CrossRef\]](#)
92. Serandrei Barbero, R.; Albani, A.D.; Bonardi, M. Ancient and Modern Salt Marshes in the Lagoon of Venice. *Palaeogeogr. Palaeoclimatol. Palaeoecol.* **2004**, *202*, 229–244. [\[CrossRef\]](#)
93. Stefani, M.; Vincenzi, S. The Interplay of Eustasy, Climate and Human Activity in the Late Quaternary Depositional Evolution and Sedimentary Architecture of the Po Delta System. *Mar. Geol.* **2005**, *222–223*, 19–48. [\[CrossRef\]](#)

-
94. Raymo, M.E.; Mitrovica, J.X. Collapse of Polar Ice Sheets during the Stage 11 Interglacial. *Nature* **2012**, *483*, 453–456. [[CrossRef](#)]
 95. Spratt, R.M.; Lisiecki, L.E. A Late Pleistocene Sea Level Stack. *Clim. Past* **2016**, *12*, 1079–1092. [[CrossRef](#)]
 96. Antonioli, F. Sea Level Change in Western-Central Mediterranean since 300 Kyr: Comparing Global Sea Level Curves with Observed Data. *Alp. Mediterr. Quat.* **2012**, *25*, 15–23.
 97. Rovere, A.; Raymo, M.E.; Vacchi, M.; Lorscheid, T.; Stocchi, P.; Gómez-Pujol, L.; Harris, D.L.; Casella, E.; O’Leary, M.J.; Hearty, P.J. The Analysis of Last Interglacial (MIS 5e) Relative Sea-Level Indicators: Reconstructing Sea-Level in a Warmer World. *Earth-Sci. Rev.* **2016**, *159*, 404–427. [[CrossRef](#)]
 98. Bini, M.; Zanchetta, G.; Drysdale, R.N.; Giaccio, B.; Stocchi, P.; Vacchi, M.; Hellstrom, J.C.; Couchoud, I.; Monaco, L.; Ratti, A.; et al. An End to the Last Interglacial Highstand before 120 Ka: Relative Sea-Level Evidence from Infreschi Cave (Southern Italy). *Quat. Sci. Rev.* **2020**, *250*, 106658. [[CrossRef](#)]
 99. Rasmussen, T.L.; Thomsen, E. Foraminifera and paleoenvironment of the Plio-Pleistocene Kallithea Bay Section, Rhodes, Greece: Evidence for cyclic sedimentation and shallow-water sapropels. In *Lagoon to Deep-Water Foraminifera and Ostracods from the Plio-Pleistocene Kallithea Bay Section, Rhodes, Greece*; Rasmussen, T.L., Hastrup, A., Thomsen, E., Eds.; Cushman Foundation for Foraminiferal Research: Fredericksburg, VA, USA, 2005; Volume 39, pp. 15–51, ISBN 9781970168341.